Suppression of epileptiform activity by high frequency sinusoidal fields in rat hippocampal slices

Marom Bikson, Jun Lian, Philip J. Hahn, William C. Stacey, Christopher Sciortino and Dominique M. Durand

Neural Engineering Center, Department of Biomedical Engineering, Case Western Reserve University, Cleveland, OH-44106, USA

(Received 10 August 2000; accepted after revision 5 October 2000)

1. Sinusoidal high frequency (20–50 Hz) electric fields induced across rat hippocampal slices were found to suppress zero-Ca^{2+}, low-Ca^{2+}, picrotoxin, and high-K^+ epileptiform activity for the duration of the stimulus and for up to several minutes following the stimulus.

2. Suppression of spontaneous activity by high frequency stimulation was found to be frequency ($<$ 500 Hz) but not orientation or waveform dependent.

3. Potassium-sensitive microelectrodes showed that block of epileptiform activity was always coincident with a stimulus-induced rise in extracellular potassium concentration during stimulation. Post-stimulus inhibition was always associated with a decrease in extracellular potassium activity below baseline levels.

4. Intracellular recordings and optical imaging with voltage-sensitive dyes showed that during suppression neurons were depolarized yet did not fire action potentials.

5. Direct injection of sinusoidal current into individual pyramidal cells did not result in a tonic depolarization. Injection of large direct current (DC) depolarized neurons and suppressed action potential generation.

6. These findings suggest that high frequency stimulation suppresses epileptiform activity by inducing potassium efflux and depolarization block.

High frequency deep brain stimulation (DBS) of certain brain structures can alleviate or completely suppress the symptoms of several neuronal disorders including Parkinson's disease (Benabid *et al.* 1994), epilepsy (Velasco *et al.* 1995, 1997) and intractable pain (Kumar *et al.* 1997). It has been suggested that high frequency DBS works by inhibiting the targeted structures (Benazzouz *et al.* 1995). However, the mechanism by which high frequency stimulation reduces excitability is unknown.

It is well established that exogenous applied fields can modulate neuronal excitability (Jefferys, 1981; Richardson & O'Reilly, 1995) and suppress epileptiform activity (Durand, 1986). Constant DC fields have been shown to suppress high-K^+- (Gluckman *et al.* 1996) and low-Ca^{2+}- (Warren & Durand, 1998; Ghai *et al.* 2000) induced epileptiform bursting by directly hyperpolarizing pyramidal neurons. While the threshold for DC inhibition is very low, electrochemical damage makes DC potentially harmful to tissue (Lilly *et al.* 1955). Furthermore, epileptiform activity returns immediately after termination of DC stimulation. Short DC pulses have been shown to inhibit high-K^+- (Jahangiri *et al.* 1996), low-Ca^{2+}- (Warren & Durand, 1998), and penicillin-induced epileptiform activity (Durand & Warman, 1994), by desynchronization of the neuronal populations. However, pulses must be critically timed and can annihilate only a single event. Bawin *et al.* (1986) showed that high frequency (60 Hz) sinusoidal fields could depress penicillin-induced epileptiform events. This effect persisted for several minutes after termination of the stimulus.

The purpose of this study was to investigate the short and long term effects of high frequency sinusoidal fields on spontaneous epileptiform activity induced in hippocampal slices. Since the stimulus artifact generated by a sinusoidal field can be easily filtered and distinguished from spontaneous activity, we were able, for the first time, to monitor extracellular and intracellular potentials during high frequency stimulation. Furthermore, we were able to obtain extracellular potassium and optical imaging measurements during field application. Our results demonstrate that high frequency stimulation can suppress spontaneous activity without triggering action potentials or requiring the release of neurotransmitters and suggest a possible mechanism for DBS inhibition.

METHODS

Preparation of hippocampal slices

All experiments were performed in the CA1 or CA3 pyramidal cell regions of hippocampal brain slices prepared from Sprague-Dawley rats (75–250 g). The experimental protocol was reviewed and approved by the Institution Animal Care and Use Committee. Rats were anaesthetized using ethyl ether and decapitated. The brain was rapidly removed and one hemisphere glued to the stage of a Vibroslicer (Vibroslice, Campden). Slicing was carried out in cold (3–4°C), oxygenated sucrose-based artificial cerebrospinal fluid (ACSF) consisting of (mM): sucrose, 220; KCl, 3; NaH_2PO_4, 1·25; $MgSO_4$, 2; $NaHCO_3$, 26; $CaCl_2$, 2; dextrose, 10. Sucrose-based slicing medium has been shown to increase cell viability *in vitro* (Aghajanian & Rasmussen, 1989). The resulting 350 μm thick slices were immediately transferred to a holding chamber containing 'normal' ACSF consisting of (mM): NaCl, 124; KCl, 3·75; KH_2PO_4, 1·25; $CaCl_2$, 2; $MgSO_4$, 2; $NaHCO_3$, 26; dextrose, 10; held at room temperature and bubbled with 95% O_2–5% CO_2.

Perfusate

After >1 h of recovery, a slice was transferred to a standard interface recording chamber with normal ACSF at $35 \pm 0{\cdot}5$°C, and a warmed, humidified 95% O_2–5% CO_2 vapour was maintained over the exposed surface of the slice. After 10 min, slices were perfused with either 'zero calcium' ACSF (zero-Ca^{2+}), 'low calcium' ACSF (low-Ca^{2+}), 'high potassium' ACSF (high-K^+), or picrotoxin-containing ACSF. Low-Ca^{2+} ACSF consisted of (mM): NaCl, 124; KCl, 4·75; KH_2PO_4, 1·25; $CaCl_2$, 0·2; $MgSO_4$, 1·5; $NaHCO_3$, 26; dextrose, 10·0. High-K^+ ACSF consisted of (mM): NaCl, 124; KCl, 8·5; NaH_2PO_4, 1·25; $CaCl_2$, 1·5; $MgSO_4$, 1·5; $NaHCO_3$, 26; dextrose, 10·0. Picrotoxin ACSF was made by adding 100 μM picrotoxin to normal ACSF (with 0·5 mM $MgSO_4$). Zero-Ca^{2+} ACSF consisted of (mM): NaCl, 124; KCl, 4·75; KH_2PO_4, 1·25; $MgSO_4$, 1·5; $NaHCO_3$, 26; dextrose, 10·0; EGTA, 1. Prolonged incubation (20–60 min) in these solutions resulted in spontaneous epileptiform activity in the CA1 or CA3 regions of the hippocampus.

Electrical recording and data analysis

Extracellular recordings of field potentials were obtained using glass micropipettes (2–5 MΩ) filled with 150 mM NaCl. One recording electrode was positioned in the somatic layer of the CA1 or CA3 region (Fig. 1). In some experiments, a second electrode was positioned at an isopotential site, in the solution, to allow for differential recording, such that the induced field artifact could be subtracted from the first electrode potential.

Intracellular recordings were obtained using sharp glass micropipettes (50–100 MΩ) filled with 2 M potassium acetate. Potassium-selective microelectrodes were constructed using established methods described elsewhere (Amman, 1986; Ghai *et al.* 2000). We utilized *N*,*N*-dimethyltrimethylsilylamine (Fluka chemicals) to silanize the electrode tips, and the Fluka 60398 potassium-selective membrane solution, which contains the potassium ionophore valinomycin. The potassium-selective microelectrodes were filled with 150 mM KCl. Electrodes were calibrated in 0·1, 1, 10, and 100 mM KCl using the separate solution method (Amman, 1986). Only electrodes of 95% Nernstian slope were used. Electrodes were at least 1000-fold selective over sodium. Potassium electrodes were placed ~100 μm below the surface of the slice in the stratum pyramidale. During intracellular and potassium measurements, the voltage recorded by a field electrode placed in the somatic layer (within 50 μm of the sharp/potassium-selective electrode) was subtracted to remove the field artifact and provide a true transmembrane/potassium measurement (Fig. 1).

All signals were subtracted and amplified with an Axoprobe-1A amplifier (Axon Instruments), low-pass filtered (1–10 Hz field and potassium, 1 kHz sharp) with a FLA-01 (Cygnus Technology, Inc., Delaware Water Gap, PA USA), and stored on videotape via an A/D converter (Sony PCM-501ES). Results are reported as means ± standard deviation; n = number of slices.

Generation and application of electric fields

Unless otherwise stated, uniform sinusoidal electric fields were generated across individual slices by passing current between two parallel AgCl-coated silver wires placed on the surface of the ACSF in the interface chamber (Fig. 1). The waveforms applied to the wires were generated by a function generator (Wavetek Arbitrary Waveform Generator 395, San Diego, CA, USA), and converted to a current by a stimulus isolation unit (A-M system analog isolator 2200). Square waves were biphasic, 100% duty cycle. The electric field (mV mm^{-1}) in the chamber was measured by two recording electrodes separated by 1 mm and calibrated to the current passed through the stimulating electrodes. Electric fields were found to be uniform across the recording chamber and were not affected by the addition of a slice.

Unless otherwise stated, slices were aligned such that the dendritic–somatic axis of the region studied (CA1 or CA3) was parallel to the direction of the induced field (0 deg). In some experiments the slices were rotated such that the dendritic–somatic axis was perpendicular to the direction of the field (90 deg).

Optical imaging with voltage-sensitive dyes

For optical imaging experiments localized fields were applied via a monopolar tungsten tip electrode positioned in the CA1 somatic layer. Optical images were obtained using established methods described elsewhere (Colom & Saggau, 1994). Briefly, prior to recording, slices were transferred to a static chamber containing 200 μM of the fluorescent probe RH414 (Molecular Probes) for 15 min. Slices were then transferred to a submerged recording chamber on an inverted microscope (Nikon). Light generated by a tungsten source was bandpass filtered and focused onto the slice through a ×10 objective. The emitted fluorescence was projected onto a photodiode array (C4675, Hamamatsu, Japan) consisting of 256 detectors arranged in a square array. Optical signals from individual photodiodes were current–voltage converted, amplified, and filtered (Yale LBC, Argo Transdata, CT, USA) before being multiplexed and digitized (12 bits) at 1 kHz (Dap 3400a, Microstar Labs, WA, USA) onto a computer (Dimension XPS H266, DELL) running custom data acquisition and signal processing software. Controls were performed to ensure the source of optical signals was extrinsic voltage-sensitive dye fluorescence rather than the intrinsic signal due to light scattering.

RESULTS

Block of epileptiform activity by high frequency stimulation

We tested the ability of 50 Hz sinusoidal fields to suppress both synaptic and non-synaptic epileptiform activity. 'Threshold' stimulation amplitude was defined as the minimum field size required to completely suppress bursting for the duration of the stimulus. Figure 2*A* shows an example of the effect of sub- and suprathreshold electric fields on spontaneous low-Ca^{2+} activity in the CA1 region. Subthreshold stimulation ($n = 17$) had no effect, resulted in a slight increase in burst duration and frequency, or

transiently suppressed activity (i.e. for a period less than the stimulation duration). Suprathreshold stimulation blocked bursting for the duration of the stimulus and for up to 4 min after termination of stimulation ($n = 29$). Application of suprathreshold fields was always associated with a 0·5–15 mV negative shift in the field potential. No long term effect on low-Ca^{2+} burst amplitude, duration or frequency was observed at any stimulus intensity or duration suggesting that the stimulation did not result in tissue damage. Epileptiform activity induced by incubation with zero-Ca^{2+} medium, with the addition of picrotoxin (100 μM) and DNQX (40 μM), was similarly blocked ($n = 3$, not shown).

Figure 2*B* shows an example of the effect of sub- and suprathreshold electric fields on spontaneous high-K^+ bursting in the CA3 region. Subthreshold stimulation had either no effect or resulted in a slight increase in burst frequency ($n = 3$). Suprathreshold stimulation blocked bursting for the duration of the stimulus and for up to 1 min after termination of stimulation ($n = 3$). As above, application of suprathreshold fields was always associated with a 0·5–15 mV negative shift in the field potential. No long term effect on high-K^+ burst amplitude, duration or frequency was observed, suggesting that the stimulation did not result in tissue damage.

Figure 2*C* shows an example of the effect of sub- and suprathreshold electric fields on picrotoxin-induced bursting. Subthreshold stimulation had no effect, resulted in a slight increase in burst duration or frequency, or transiently suppressed activity ($n = 8$). Suprathreshold stimulation blocked bursting for the duration of the stimulus and for up to 2 min after termination of stimulation ($n = 11$) and was always coincident with a 0·5–15 mV shift in the field potential.

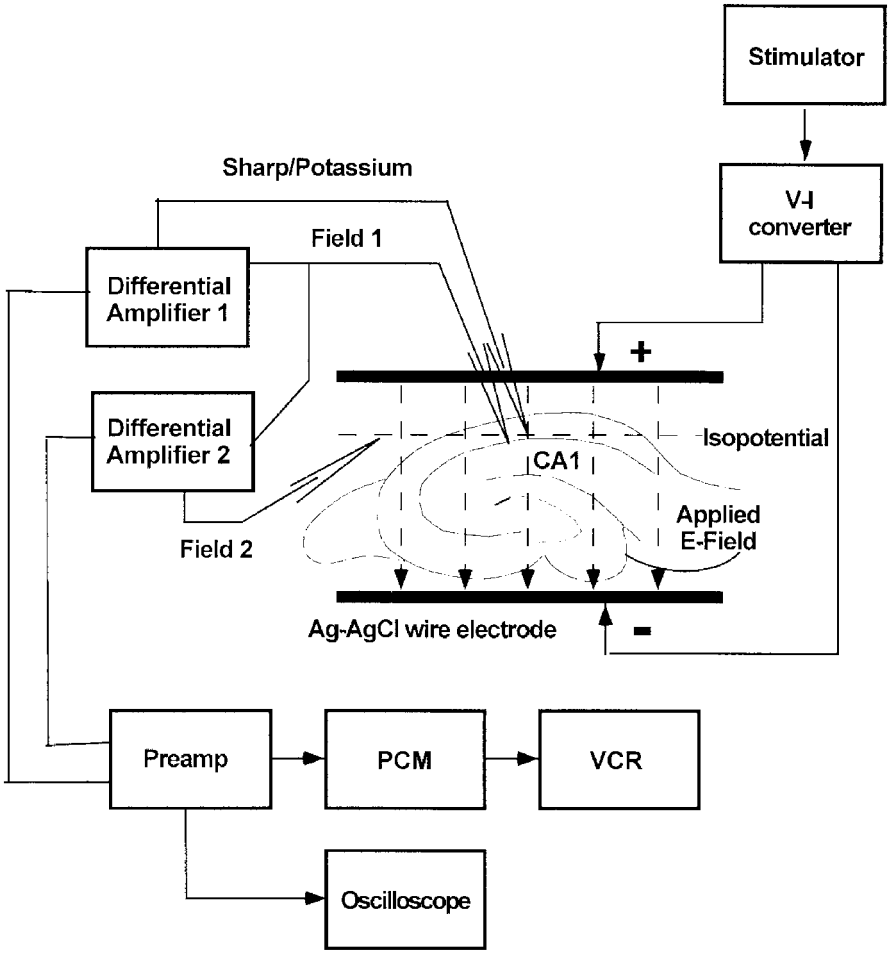

Figure 1. Experimental setup for application of uniform sinusoidal fields across hippocampal slices

Uniform electric fields were generated by passing current between two parallel AgCl-coated silver wires. Spontaneous epileptiform activity was monitored with a field electrode (Field 1) positioned in the stratum pyramidale. The stimulus artifact was removed from the field recording either by low-pass filtering or by subtraction of the voltage recorded at an isopotential (Field 2). In experiments including intracellular (Sharp) or ion-selective (Potassium) recordings, the voltage recorded at a proximal field electrode (Field 1) was subtracted to remove the field artifact and produce a true transmembrane or potassium measurement.

Effect of stimulus frequency, waveform and slice orientation

The effect of stimulus frequency on field efficacy was examined by determining the threshold for suppression of spontaneous low-Ca^{2+} bursting using 20, 50, 500 and 5000 Hz sinusoidal fields. Electric fields were applied for 2 min. No significant difference was found in the threshold for suppression using 20 Hz (113 ± 41 mV mm^{-1}, $n = 4$) and 50 Hz (144 ± 36 mV mm^{-1}, $n = 11$) stimulation (Fig. 3*A*). The efficacy of lower frequency (< 15 Hz) fields could not be tested because the stimulus artifact could not be filtered without attenuation of the activity. Sinusoidal fields of 500 Hz (Fig. 3*B*) and 5000 Hz were found to be ineffective at suppressing activity at any field strength tested (20–300 mV mm^{-1}, $n = 3$).

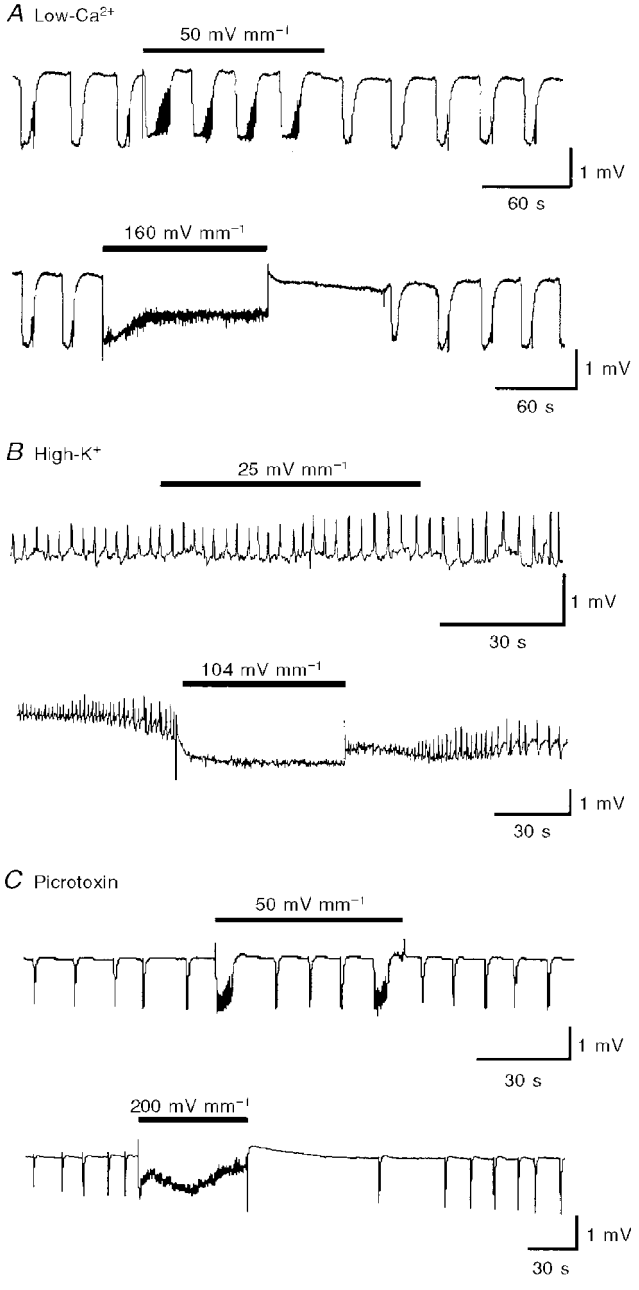

Figure 2. Suppression of synaptic and non-synaptic epileptiform activity by high frequency stimulation

Effect of sub- (top) and suprathreshold (bottom) 50 Hz sinusoidal fields on spontaneous activity induced by perfusion of slices with low-Ca^{2+} ACSF (*A*), high-K^+ ACSF (*B*) and picrotoxin ACSF (*C*). In this and all subsequent figures the horizontal bars indicate the duration of field application.

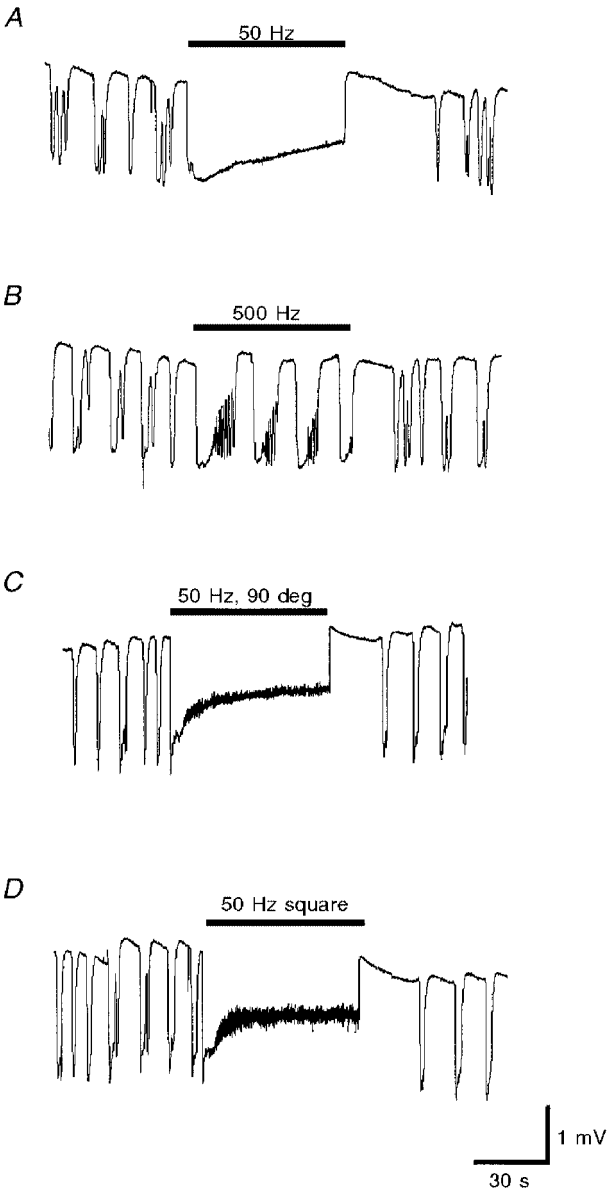

Figure 3. Effect of field frequency, waveform and orientation on suppression threshold

A–D, 200 mV mm^{-1} fields were applied during spontaneous low-Ca^{2+}-induced bursting. *A*, 50 Hz sinusoidal field suppressed low-Ca^{2+} activity in a hippocampal slice oriented at 0 deg relative to the imposed field (see Methods). *B*, in the same slice, 500 Hz fields were ineffective at blocking activity. *C*, block of activity by 50 Hz sinusoidal fields after the slice was rotated 90 deg. *D*, block of low-Ca^{2+}-induced bursting in the same hippocampal slice by 50 Hz square wave field.

To test the effect of field orientation on blocking threshold, the efficacy of fields applied at 0 and 90 deg relative to the dendritic–somatic axis were compared (Fig. 3*C*). The mean threshold to block low-Ca^{2+} bursting in slices rotated 90 deg (128 ± 19 mV mm^{-1}, $n = 3$) was not significantly different from 0 deg controls. Similarly, the mean threshold to block low-Ca^{2+} bursting using a 50 Hz square waveform (99 ± 34 mV mm^{-1}, $n = 6$; Fig. 3*D*) was not significantly different from the sinusoidal controls, suggesting that the stimulus waveform does not affect field efficacy.

Effect of high frequency stimulation on $[K^+]_o$

The effect of high frequency stimulation on extracellular potassium was studied using ion-sensitive microelectodes. During low-Ca^{2+} bursting, subthreshold stimulation had either no effect or resulted in a small increase in extracellular potassium and a transient disruption of spontaneous activity (Fig. 4*A*, $n = 3$). However, as the extracellular potassium concentration decayed, bursting was re-initiated. Suprathreshold stimulation (Fig. 4*B*) resulted in a larger increase ($2{\cdot}2 \pm 0{\cdot}4$ mM, $n = 3$) in extracellular potassium activity which decayed at a slower rate ($n = 3$). Termination of stimulation was followed by a transient decrease in extracellular potassium concentration below the baseline level, during which activity was suppressed. Bursting resumed as extracellular potassium levels returned to baseline. Application of sub- and suprathreshold stimulation

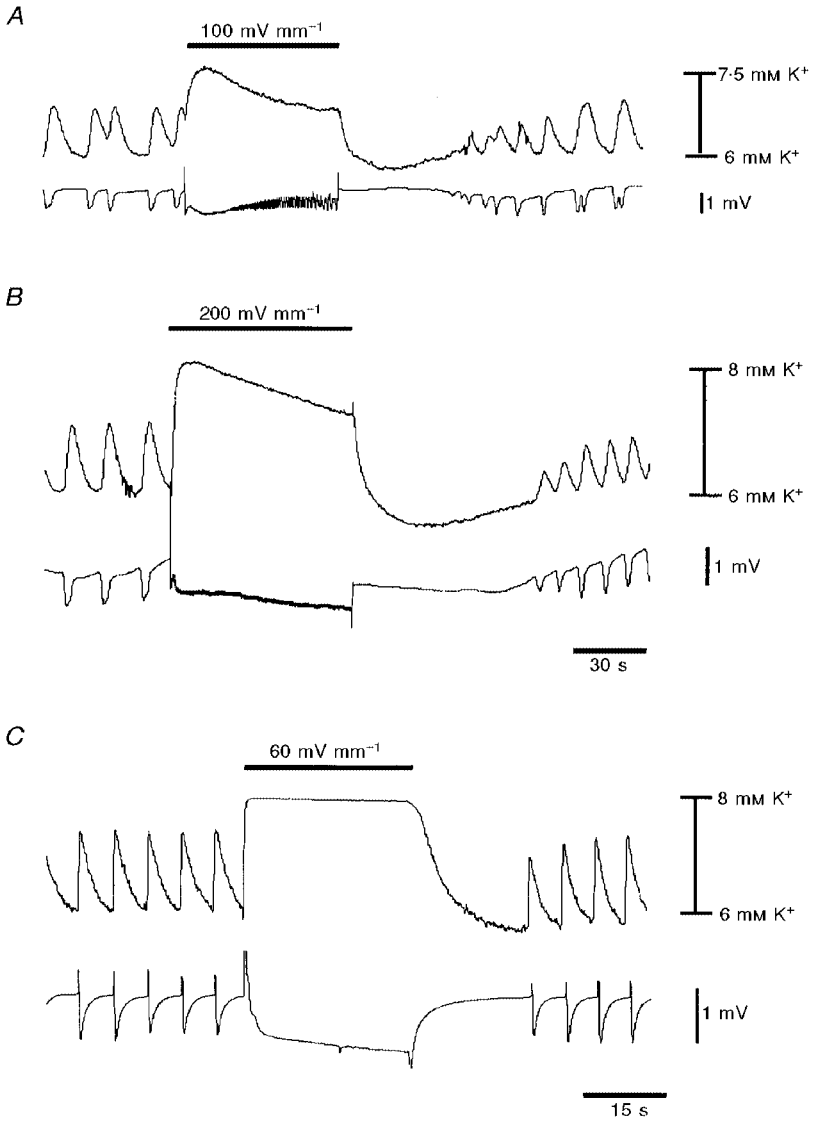

Figure 4. Extracellular potassium measurements during attempts to suppress activity with 50 Hz sinusoidal fields

A, during low-Ca^{2+} epileptiform activity, subthreshold stimulation resulted in a transient increase in extracellular potassium. As the potassium increase decayed, spontaneous activity resumed. *B*, in the same slice, application of suprathreshold stimulation resulted in a larger potassium increase during stimulation and suppression of activity. *C*, during picrotoxin epileptiform activity suprathreshold stimulation resulted in similar transients in extracellular potassium.

during picrotoxin-induced bursting resulted in similar transients in extracellular potassium concentration (Fig. 4*C*, $n = 3$).

Effect of high frequency stimulation on transmembrane potential

We investigated the effect of high frequency stimulation on membrane potential and action potential frequency using sharp intracellular recording. During picrotoxin-induced bursting subthreshold stimulation did not interfere with field or intracellular burst generation (not shown, $n = 4$). Suprathreshold stimulation blocked bursting (Fig. 5*A*) and resulted in a tonic depolarization (19 ± 5 mV, $n = 7$) in the membrane potential (Fig. 5*B*). While the initiation of field application was associated with the generation of several action potentials, no subsequent action potentials were observed during the duration of the suprathreshold stimulation. The tonic depolarization is seen more clearly after low-pass filtering (Fig. 5*C*). The transient peak observed, after low-pass filtering, at the initiation of stimulation is consistent with the generation of action potentials only during the first few seconds of stimulation.

Optical imaging of membrane polarization during high frequency stimulation

To determine the direction of membrane polarization during high frequency stimulation and obtain a spatial map of this polarization we employed optical imaging with voltage-sensitive dyes ($n = 3$). Voltage-sensitive dyes provide a direct measurement of transmembrane voltage changes (Grinvald *et al.* 1988). Application of 50 Hz 1 mA stimulation resulted in a global tonic depolarization for the duration of the stimulation (Fig. 6). Consistent with data from intracellular measurements, an additional transient depolarization was observed at the initiation of stimulation. A grey-scale spatial map shows that the depolarization initiated and terminated almost simultaneously throughout the CA1 region (Fig. 6*C*), suggesting that the polarization was not propagating from the stimulation site. Depolarization was observed in the stratum oriens, stratum pyramidale, and

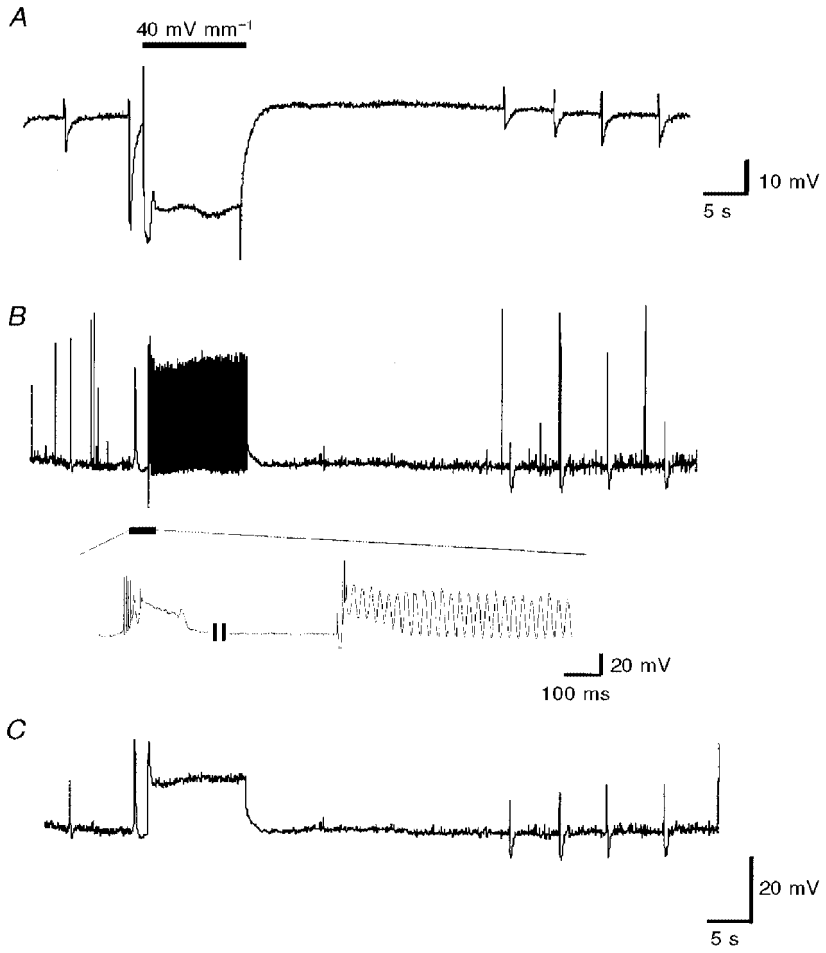

Figure 5. Simultaneous field and transmembrane potential recordings during application of a suprathreshold 50 Hz sinusoidal field

A, field recordings were low-pass filtered at 10 Hz. *B*, the unfiltered transmembrane potential was obtained by subtracting the sharp intracellular from the field potential. It is unclear what component of the measured 50 Hz oscillation is residual field artifact and what represents true oscillations in the transmembrane potential. *C*, filtration of *B* by additional 10 Hz filter shows that during field application the neuron was depolarized by ~20 mV.

stratum radiatum indicating that cell bodies as well as dendrites were all depolarized by the sinusoidal field.

Intracellular stimulation with sinusoidal current

Consistent with previous studies (Garcia-Munoz *et al.* 1993; Leung & Yu, 1998), direct injection of small sinusoidal currents (20–50 Hz, < 0·5 nA) into a single CA1 pyramidal cell produced oscillations in the membrane potential but did not result in a tonic depolarization (Fig. 7*A*, $n = 8$). Larger sinusoidal current (20–50 Hz, 0·5–3 nA) resulted in more robust oscillations, still centred around the resting membrane potential, and triggered action potentials (Fig. 7*B*, $n = 8$).

Consistent with earlier studies (Hablitz & Johnston, 1981; Wong & Prince, 1981) injection of small DC (< 2 nA) depolarized neurons and triggered action potentials. Injection of larger DC (3–4 nA) further depolarized cells and suppressed action potential generation (Fig. 7*C*, $n = 5$).

DISCUSSION

Mechanism of block

The lack of action potential generation during high frequency block rules out the possibility that the stimulation is simply pacing neurons. It has been suggested that high frequency stimulation can produce neuronal inhibition by a mechanism linked to neurotransmitter release (Benazzouz *et al.* 1995). However, the suppression of epileptiform activity in low-Ca^{2+} and zero-Ca^{2+} solutions, during which synaptic transmission is blocked (Jones & Heinemann, 1987), and in the presence of post-synaptic receptor antagonists, suggests that transmitter release is not necessary for high frequency block. High frequency stimulation has been shown to suppress the conduction of action potentials along axons (Bowman & McNeal, 1986). However, the frequencies required for block of conduction (> 2 kHz) are inconsistent with the findings that lower frequencies (< 150 Hz) are required for suppression of epileptiform activity.

Since direct injection of sinusoidal current into individual cells did not result in a tonic depolarization shift, the neuronal depolarization observed during successful block of spontaneous activity must be due to a network effect (compare Figs 5 and 7*B*). It is well established that high frequency stimulation is associated with an increase in extracellular potassium (Gardner-Medwin, 1983; Bawin *et al.* 1986; Poolos *et al.* 1987; Kaila *et al.* 1997). The effect of subthreshold stimulation on the epileptiform event waveform (Fig. 2) is consistent with moderate increases in extracellular potassium activity (Rutecki *et al.* 1985; Bikson *et al.* 1999). While small increases in potassium can promote epileptiform activity, large increases can suppress spontaneous bursting (Rutecki *et al.* 1985). An increase in extracellular potassium is expected to depolarize cells and could lead to the

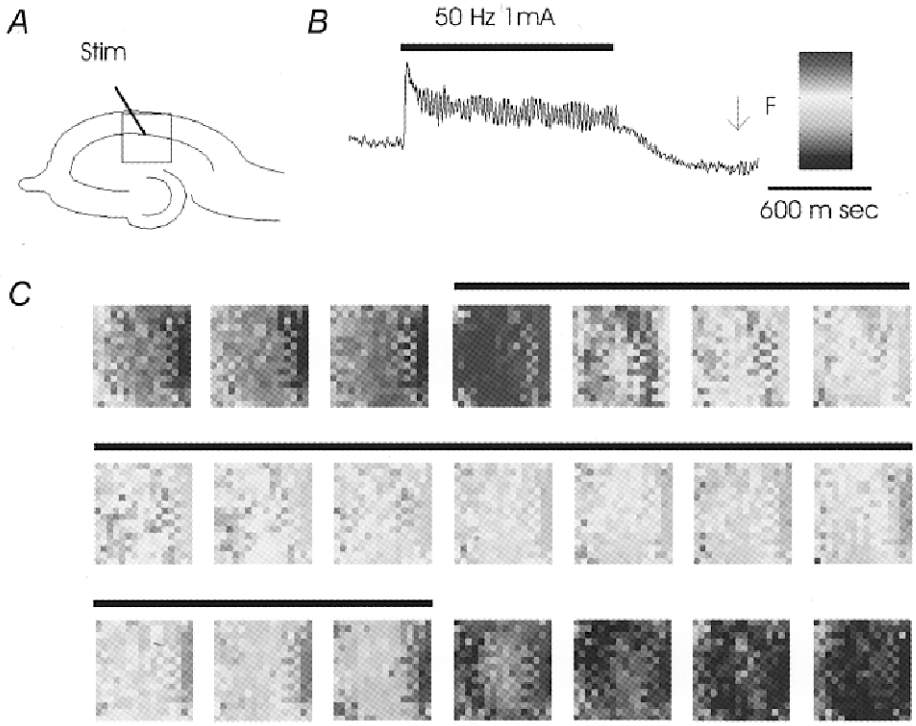

Figure 6. Optical imaging with voltage-sensitive dyes during high frequency sinusoidal stimulation

A, schematic representation of projection of slice onto 16 × 16 element photodiode array and location of monopolar stimulation electrode (Stim). *B*, optical signal from signal channel photodiode. Fluorescence decreases with increases in membrane potential. An example of the grey-scale code assigned to each individual channel at full scale is shown on the right. *C*, spatial map using grey-scale assignments. Each frame is separated by 80 ms.

disruption of epileptiform activity by depolarization block (Poolos *et al.* 1987).

Depolarization block is induced when persistent membrane depolarization results in the tonic inactivation of Na^+ channels such that action potentials cannot be initiated (Hille, 1992). Consistent with modelling studies (Traub *et al.* 1991; Pinsky & Rinzel, 1994) we found that a depolarization of > 20 mV was sufficient to induce depolarization block. During application of suprathreshold sinusoidal electric fields neurons were depolarized above this level and thus were prevented from firing action potentials (compare Figs 5 and 7*C*).

In this study, suprathreshold stimulation was always associated with a rise in extracellular potassium (~2 mM) and a negative field shift. The negative field shift is consistent with the removal of excess extracellular potassium by spatial buffering mechanisms (Bikson *et al.* 1999). An increase in extracellular potassium of 6 mM would be sufficient to suppress spontaneous activity and depolarize neurons by ~20 mV (Hille 1992; Hahn & Durand, 1998). Potassium-selective microelectrodes measure an average potassium concentration at the interface of the bath and slice surface, and so underestimate the potassium concentration at the surface of the cells during endogenous potassium release. Current-clamp (Takahashi & Tsuruhara, 1987) and voltage-clamp (Chvatal *et al.* 1999) recordings from glial cells, as well as modelling studies (Hounsgaard & Nicholson, 1983), approximate this underestimate at 25–75%. Thus, in this study, the 2 mM increase measured by potassium-selective electrodes during suprathreshold stimulation is consistent with an ~6 mM rise at the surface of cells, which would result in depolarization block.

Orientation dependence

Previously, it has been shown that DC fields suppress epileptiform activity in an orientation-dependent manner (Ghai *et al.* 1998). This is consistent with the hypothesis that DC fields suppress activity by directly polarizing cells

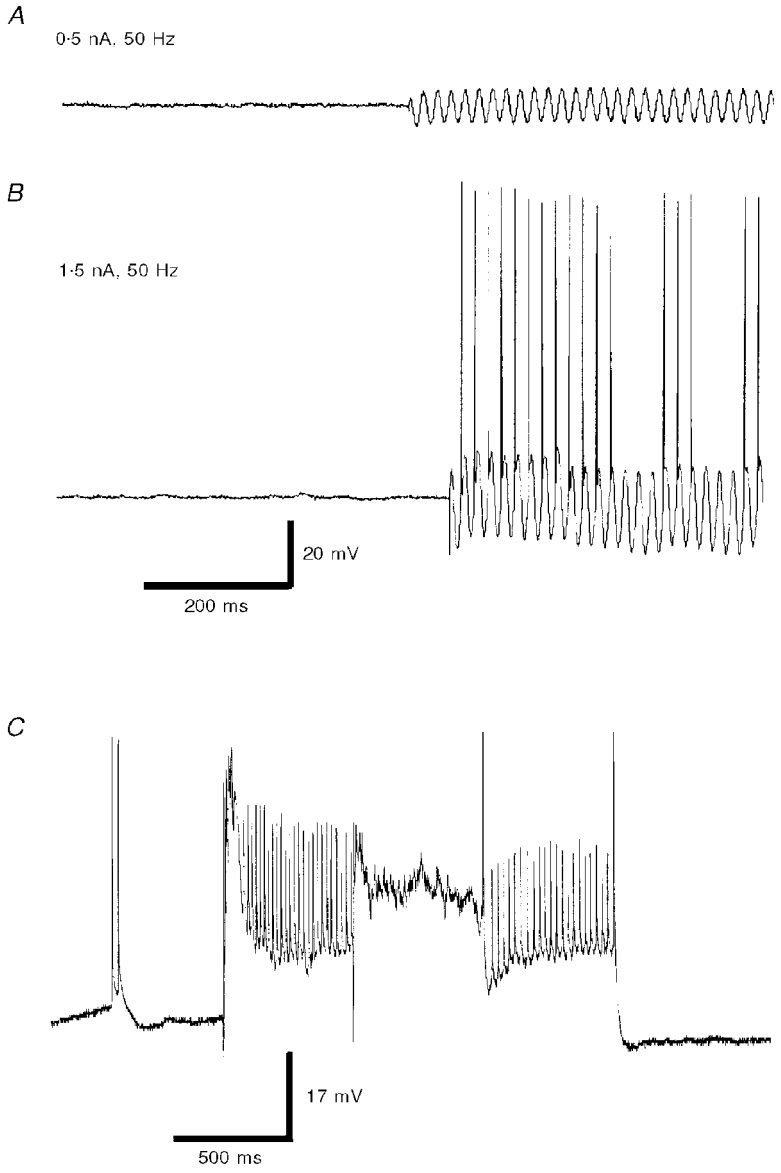

Figure 7. Injection of direct and sinusoidal currents into a single neuron

A, response of CA1 pyramidal cell to injection of 0·5 nA, 50 Hz sinusoidal current. *B*, response of same cell to injection of 1·5 nA, 50 Hz sinusoidal current. *C*, response of CA1 pyramidal cell to different levels of DC injection. First step 2 nA, second step 3·5 nA, third step 2 nA.

(Jefferys, 1981; Chan *et al.* 1988; Gluckman *et al.* 1996). The insensitivity of AC field suppression threshold to slice orientation suggests that the activity is not suppressed by direct polarization of pyramidal cell somas. This represents an advantage over DC stimulation since all cells exposed to a high frequency field, not just those oriented parallel to the induced field, would be affected by stimulation (Kayyali & Durand, 1991; Gluckman *et al.* 1996; Warren & Durand, 1998).

Mechanism of the extracellular potassium increase

Since neurons were found to fire action potentials only at the initiation of suprathreshold high frequency stimulation, it is of interest to speculate on the source of the potassium transients associated with suppression. The tonic increase in extracellular potassium could reflect enhanced potassium efflux, a disruption of potassium clearance mechanisms, or a combination of both. Glial cells have been shown to play a critical role in extracellular potassium homeostasis (Amedee *et al.* 1997). Drugs that affect glial potassium buffering mechanisms have been shown to modulate stimulus-induced potassium efflux (Gabriel *et al.* 1998). Chvatal *et al.* (1999) showed that injection of current into individual glial cells can induce large (>30 mM) increases in extracellular potassium. Unlike pyramidal neurons, glial cells are orientated randomly across the hippocampus. Thus, the insensitivity of suppression threshold to slice orientation (Fig. 3) is consistent with an action on glial cells.

Preliminary experiments indicate that bath application of TTX induces a small (~1 mM) increase in baseline potassium and suppresses field-induced potassium rises ($n = 3$, data not shown). Several factors could contribute to this TTX sensitivity. The brief burst of pyramidal cell action potentials observed at the start of stimulation could be necessary to initiate a potassium rise. Once depolarized by an increase in extracellular potassium, outward potassium currents in pyramidal cells would remain high even in the absence of action potentials (Hahn & Durand, 1998; Muller & Somjen, 2000). In this scheme, stimulation of glial cells could further contribute to potassium efflux or disrupt glial potassium clearance mechanisms (Amedee *et al.* 1997). Alternatively, TTX might affect glial function by directly antagonizing glial sodium channels (Nowak *et al.* 1987) or indirectly interfering with Na^+–K^+ pump activity and thus potassium homeostasis (Xiong & Stringer, 2000). The moderate increase in baseline potassium observed after addition of TTX is consistent with this idea. A fourth explanation for TTX sensitivity could be a contribution to the potassium rise from spiking cells not recorded in this study, such as interneurons or axons of passage. The stimulation threshold for these structures would also be insensitive to slice orientation.

Recovery of spontaneous activity

Previous attempts to suppress spontaneous epileptiform activity using constant DC fields have suffered from the 'rebound block phenomena', where the removal of the inhibitory stimulus immediately triggers the reinitiation of bursting (Ghai *et al.* 2000). Using high frequency fields spontaneous activity could be suppressed for up to several minutes after the termination of stimulation. The post-stimulus refractory period was consistent with the depression of potassium below baseline levels (Rutecki *et al.* 1985). The findings suggests that low-duty cycle stimulation protocols can be developed that will suppress activity by alternating between during-stimulus and post-stimulus inhibitory mechanisms.

Conclusions: clinical relevance

Taken together these results suggest that high frequency stimulation inhibits epileptiform activity by the modulation of extracellular potassium concentration and depolarization block.

Despite extensive clinical application in the treatment of epilepsy and Parkinson's disease, the effect of high frequency stimulation on CNS tissue is largely unknown. Paradoxically, high frequency stimulation mimics the effect of lesioning a structure, suggesting that DBS is inhibiting the targeted region (Benazzouz *et al.* 1995). The results of this study suggest a mechanism by which high frequency stimulation could decrease neuronal excitability. While there are clear differences between clinical DBS and our experimental protocol, several *in vivo* observations such as the effectiveness of stimulation in a narrow frequency band (Benabid *et al.* 1991; Mirski *et al.* 1997), a tonic shift in the EEG during stimulation (Velasco *et al.* 1997), a pre-suppression facilitation (Ashby *et al.* 1999), and a post-stimulus refractory period (Benazzouz *et al.* 1995; Ashby *et al.* 1999) are reproduced by our *in vitro* model.

Aghajanian, G. K. & Rasmussen, K. (1989). Intracellular studies in the facial nucleus illustrating a simple new method for obtaining viable motoneurons in adult rat brain slices. *Synapse* **3**, 331–338.

Amedee, T., Robert, A. & Coles, J. A. (1997). Potassium homeostasis and glial energy metabolism. *Glia* **21**, 46–55.

Amman, D. (1986). *Ion-selective Microelectrodes: Principles, Design and Application*. Springer-Verlag, Berlin, Heidelberg, New York and Tokyo.

Ashby, P., Kim, Y. J., Kumar, R., Lang, A. E. & Lozano, A. M. (1999). Neurophysiological effects of stimulation through electrodes in the human subthalamic nucleus. *Brain* **122**, 1919–1931.

Bawin, S. M., Abu-Assal, M. L., Sheppard, A. R., Mahoney, M. D. & Adey, W. R. (1986). Long-term effects of sinusoidal extracellular electric fields in penicillin-treated rat hippocampal slices. *Brain Research* **399**, 194–199.

Benabid, A. L., Pollak, P., Gervason, C., Hoffman, D., Gao, D. M., Hommel, M., Perret, J. E. & Rougemont, J. D. (1991). Long-term suppression of tremor by chronic stimulation of the ventral intermediate thalamic nucleus. *Lancet* **337**, 403–406.

Benabid, A. L., Pollak, P., Gross, C., Hoffman, D., Benazzouz, A., Gao, D. M., Laurent, A., Gentil, M. & Perret, J. (1994). Acute and long-term effects of subthalamic nucleus stimulation in Parkinson's disease. *Stereotactic and Functional Neurosurgery* **62**, 76–84.

Benazzouz, A., Piallat, B., Pollak, P. & Benabid, A. (1995). Responses of substantia nigra pars reticulata and globus pallidus complex to high frequency stimulation of the subthalamic nucleus in rats: electrophysiological data. *Neuroscience Letters* **189**, 77–80.

Bikson, M., Ghai, R. S., Baraban, S. C. & Durand, D. M. (1999). Modulation of burst frequency, duration, and amplitude in the zero-Ca^{2+} model of epileptiform activity. *Journal of Neurophysiology* **82**, 2262–2270.

Bowman, B. R. & McNeal, D. R. (1986). Response of singla alpha motorneurons to high frequency pulse trains. *Applied Neurophysiology* **49**, 121–138.

Chan, C. Y., Hounsgaard, J. & Nicholson, C. (1988). Effects of electric fields on transmembrane potential and excitability of turtle cerebellar Purkinje cells *in vitro*. *Journal of Physiology* **402**, 751–771.

Chvatal, A., Anderova, M., Ziak, D. & Sykova, E. (1999). Glial depolarization evokes a larger potassium accumulation around oligodendrocytes than around astrocytes in gray matter of rat spinal cord slices. *Journal of Neuroscience Research* **56**, 493–505.

Colom, L. V. & Saggau, P. (1994). Spontaneous interictal-like activity originates in multiple areas of the CA2-CA3 region of hippocampal slices. *Journal of Neurophysiology* **71**, 1574–1585.

Durand, D. (1986). Electrical stimulation can inhibit synchronized neuronal activity. *Brain Research* **382**, 139–144.

Durand, D. M. & Warman, E. N. (1994). Desynchronization of epileptiform activity by extracellular current pulses in rat hippocampal slices. *Journal of Physiology* **480**, 527–537.

Gabriel, S., Kivi, A., Eilers, A., Kovacs, R. & Heinemann, U. (1998). Effects of barium on stimulus-induced rises in $[K^+]_o$ in juvenile rat hippocampal area CA1. *NeuroReport* **9**, 2583–2587.

Garcia-Munoz, A., Barrio, L. C. & Buno, W. (1993). Membrane potential oscillations in CA1 hippocampal pyramidal neurons *in vitro*: intrinsic rhythms and fluctuations entrained by sinusoidal injected current. *Experimental Brain Research* **97**, 325–333.

Gardner-Medwin, A. R. (1983). A study of the mechanisms by which potassium moves through brain tissue in the rat. *Journal of Physiology* **335**, 353–374.

Ghai, R. S., Bikson, M. & Durand, D. M. (1998). Electric field suppression of low calcium epileptiform activity in the rat brain. *Society for Neuroscience Abstracts* **24**, 1213.

Ghai, R. S., Bikson, M. & Durand, D. M. (2000). Effects of applied electric fields on low-calcium epileptiform activity in the CA1 region of rat hippocampal slices. *Journal of Neurophysiology* **84**, 274–280.

Gluckman, B. J., Neel, E. J., Netoff, T. I., Ditto, W. L., Spano, M. L. & Schiff, S. J. (1996). Electric field suppression of epileptiform activity in hippocampal slices. *Journal of Neurophysiology* **76**, 4202–4205.

Grinvald, A., Frostig, R. D., Lieke, E. & Hildesheim, R. (1988). Optical imaging of neuronal activity. *Physiological Reviews* **68**, 1285–1358.

Hablitz, J. J. & Johnston, D. (1981). Endogenous nature of spontaneous bursting in hippocampal pyramidal neurons. *Cellular and Molecular Neurobiology* **1**, 325–334.

Hahn, P. J. & Durand, D. M. (1998). Dynamics of neuronal activity in high potassium. *Annals of Biomedical Engineering* **26**, S-93.

Hille, B. (1992). *Ionic Channels of Excitable Membranes*. Sinauer, Sunderland, USA.

Hounsgaard, J. & Nicholson, C. (1983). Potassium accumulation around individual Purkinje cells in cerebellar slices from the guinea-pig. *Journal of Physiology* **340**, 359–388.

Jahangiri, A., Durand, D. M. & Lin, J. C. (1996). Phase resetting of high potassium spiking activity in hippocampal slices. *Society for Neuroscience Abstracts* **22**, 972, 387.1.

Jefferys, J. G. R. (1981). Influence of electric fields on the excitability of granule cells in guinea-pig hippocampal slices. *Journal of Physiology* **319**, 143–152.

Jones, R. S. G. & Heinemann, U. (1987). Abolition of the orthodromically evoked IPSP of CA1 pyramidal cells before the EPSP during washout of calcium from hippocampal slices. *Experimental Brain Research* **65**, 676–680.

Kaila, K., Lamsa, K., Smirnov, S., Taira, T. & Voipio, J. (1997). Long-lasting GABA-mediated depolarization evoked by high-frequency stimulation in pyramidal neurons of rat hippocampal slice is attributable to a network-driven, bicarbonate-dependent K^+ transient. *Journal of Neuroscience* **17**, 7662–7672.

Kayyali, H. & Durand, D. (1991). Effects of applied currents on epileptiform bursts *in vitro*. *Experimental Neurology* **113**, 249–254.

Kumar, K., Toth, C. & Nath, R. K. (1997). Deep brain stimulation for intractable pain: a 15-year experience. *Neurosurgery* **40**, 736–746.

Leung, L. S. & Yu, H. (1998). Theta-frequency resonance in hippocampal CA1 neurons *in vitro* demonstrated by sinusoidal current injection. *Journal of Neurophysiology* **79**, 1592–1596.

Lilly, J. C., Hughes, J. R., Alvord, E. C. & Garkin, T. W. (1955). Brief non-injurious waveforms for stimulation of the brain. *Science* **121**, 468–469.

Mirski, M. A., Rossell, L. A., Terry, J. B. & Fisher, R. S. (1997). Anticonvulsant effect of anterior thalamic high frequency electrical stimulation in the rat. *Epilepsy Research* **28**, 89–100.

Muller, M. & Somjen, G. G. (2000). Na(+) and K(+) concentrations, extra- and intracellular voltages, and the effect of TTX in hypoxic rat hippocampal slices. *Journal of Neurophysiology* **83**, 735–745.

Nowak, L., Ascher, P. & Berwald-Netter, Y. (1987). Ionic channels in mouse astrocytes in culture. *Journal of Neuroscience* **7**, 101–109.

Pinsky, P. F. & Rinzel, J. (1994). Intrinsic and network rhythmogensis in reduced Traub model for CA3 neurons. *Journal of Computational Neuroscience* **1**, 39–60.

Poolos, N. P., Mauk, M. D. & Kocsis, J. D. (1987). Activity-evoked increases in extracellular potassium modulate presynaptic excitability in the CA1 region of the hippocampus. *Journal of Neurophysiology* **58**, 404–416.

Richardson, T. L. & O'Reilly, C. N. (1995). Epileptiform activity in the dentate gyrus during low-calcium perfusion and exposure to transient electric fields. *Journal of Neurophysiology* **74**, 388–399.

Rutecki, P. A., Lebeda, F. J. & Johnston, D. (1985). Epileptiform activity induced by changes in extracellular potassium in hippocampus. *Journal of Neurophysiology* **54**, 1363–1374.

Takahashi, T. & Tsuruhara, H. (1987). Slow depolarizing potentials recorded from glial cells in the rat superficial dorsal horn. *Journal of Physiology* **388**, 597–610.

Traub, R. A., Wong, R. K. S., Miles, R. & Michelson, H. (1991). A model of a CA3 hippocampal pyramidal neuron incorporating voltage-clamp data of intrinsic conductances. *Journal of Neurophysiology* **66**, 635–650.

Velasco, F., Velasco, M., Velasco, A. L., Jimenez, F., Marquez, I. & Rise, M. (1995). Electrical stimulation of the centromedian thalamic nucleus in control of seizures: long-term studies. *Epilepsia* **36**, 63–71.

Velasco, M., Velasco, F., Velasco, A. L., Brito, F., Jimenez, F., Marquez, I. & Rojas, B. (1997). Electrocortical and behavioral responses produced by acute electrical stimulation of the human centromedian thalamic nucleus. *Electroencephalography and Clinical Neurophysiology* **102**, 461–471.

Warren, R. J. & Durand, D. M. (1998). Effects of applied currents on spontaneous epileptiform activity induced by low calcium in the rat hippocampus. *Brain Research* **806**, 186–195.

Wong, R. K. & Prince, D. A. (1981). Afterpotential generation in hippocampal pyramidal cells. *Journal of Neurophysiology* **45**, 86–97.

Xiong, Z. & Stringer, J. L. (2000). Sodium pump, not glial spatial buffering, clears potassium after epileptiform activity induced in the dentate gyrus. *Journal of Neurophysiology* **83**, 1443–1451.

Acknowledgements

Financial support for this work was provided by the Whitaker Foundation and the National Institutes of Health.

Corresponding author

D. M. Durand: Department of Biomedical Engineering, 3510 Charles B. Bolton Building, Case Western Reserve University, 10900 Euclid Avenue, Cleveland, OH-44106, USA.

Email: dxd6@po.cwru.edu